

## Supplementary Information

*Viral Infection of the Tumor Microenvironment Mediates Antitumor Immunotherapy via Selective TBK1-IRF3 Signaling*

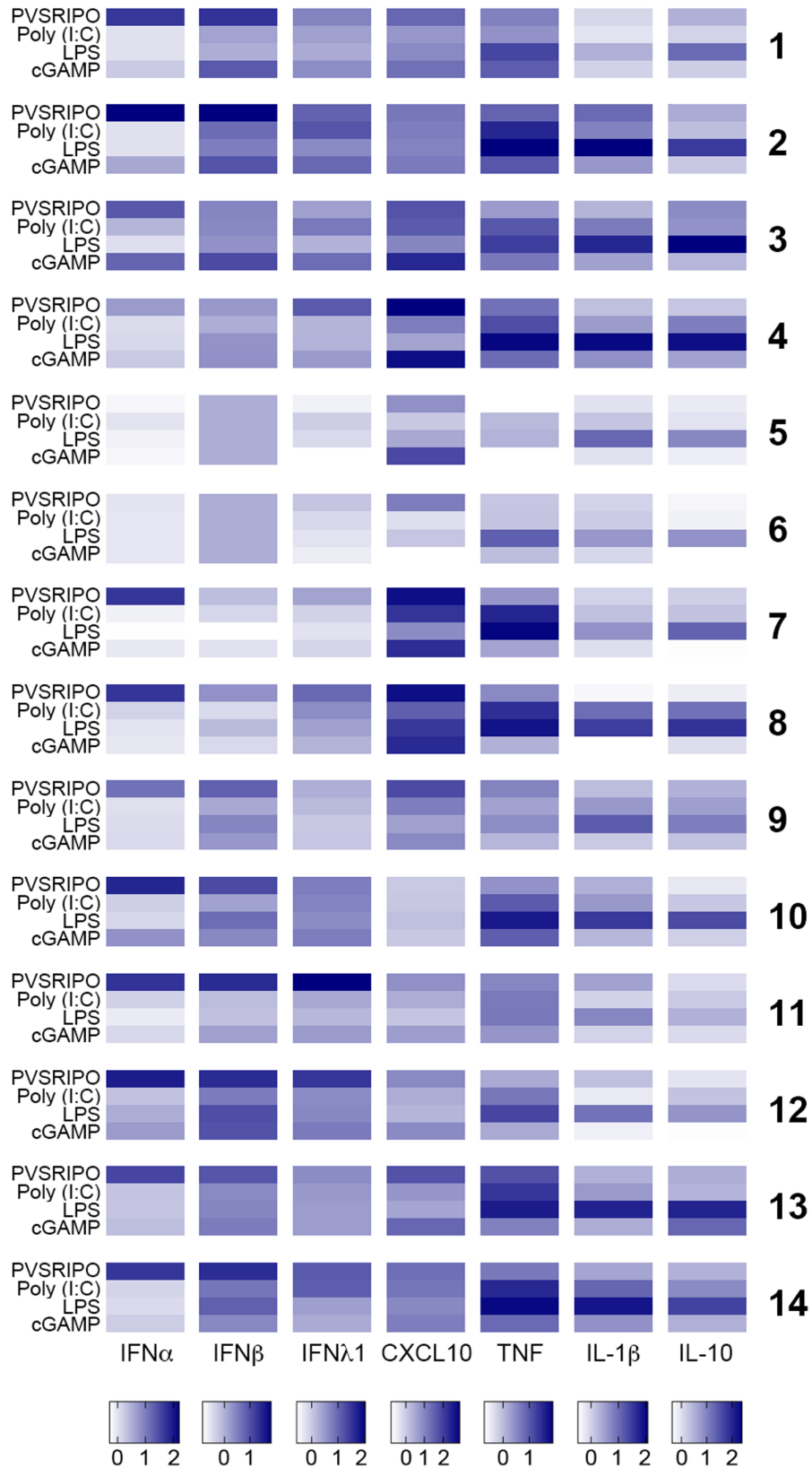
Brown *et al.*



**Supplementary Figure 1, related to Figure 1b. Representative gating strategy for analysis of CD155 expression distribution in GBM tumor specimens.**

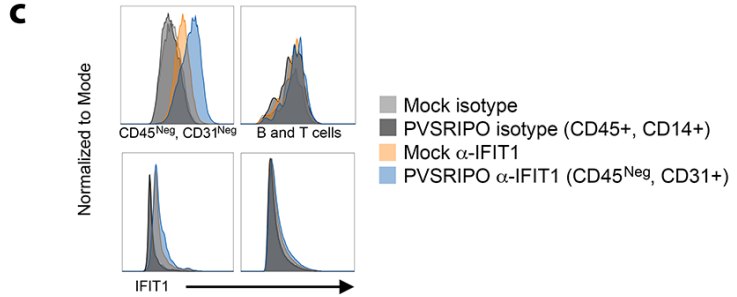
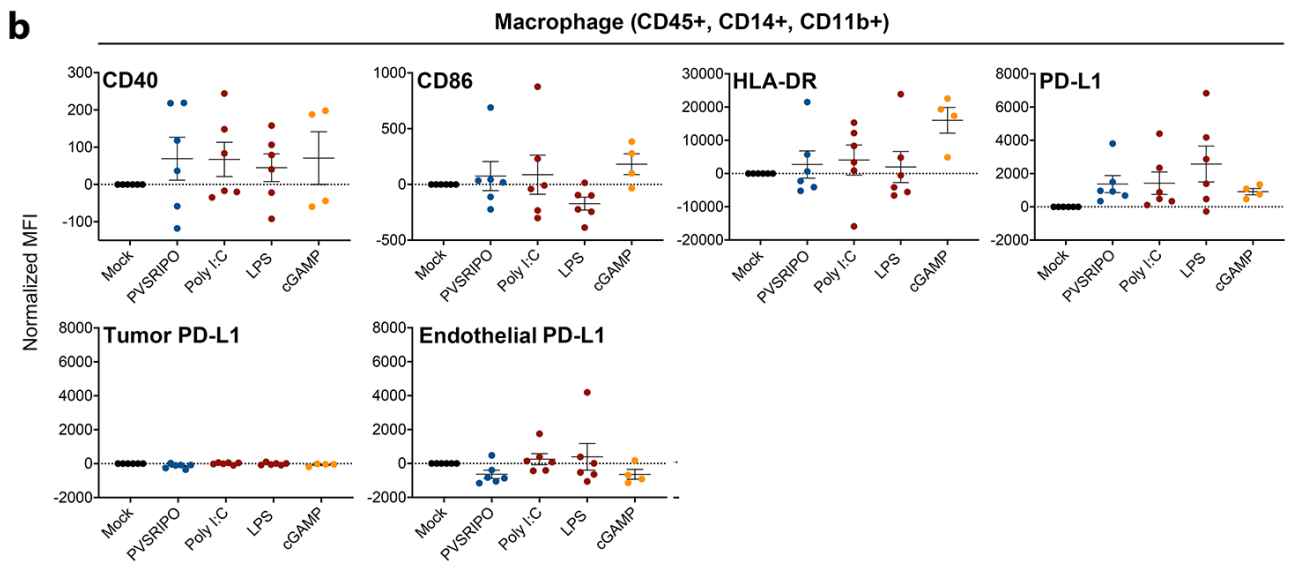
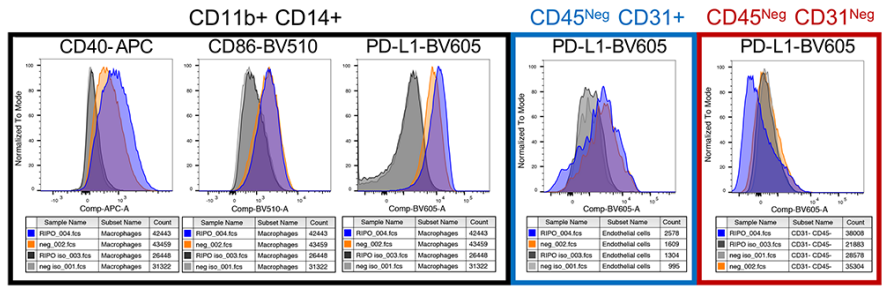
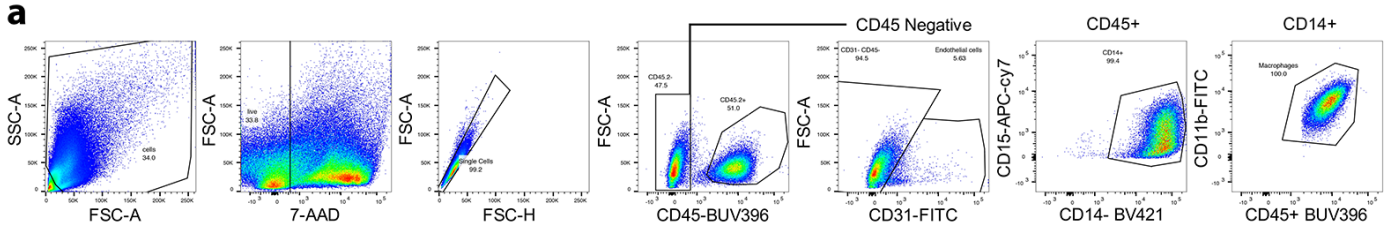
Red histograms are fluorescence minus one isotype control-PE antibody stained, light blue histograms are CD155-PE stained. Bottom 2 panels show comparison of CD14 expression in microglia and macrophages.

## GBM tissue-matched cytokine induction



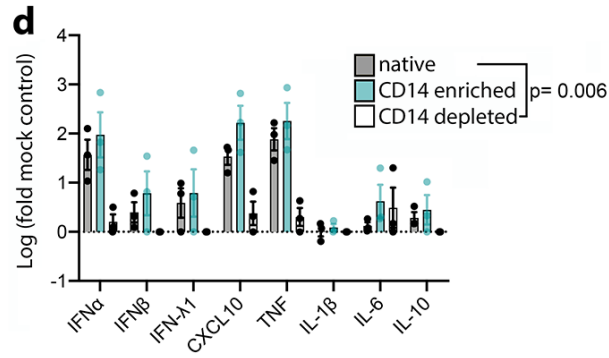
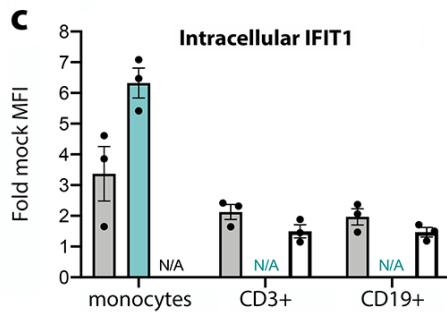
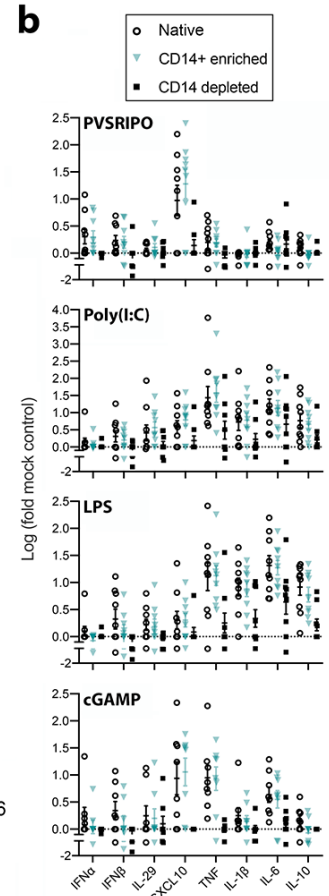
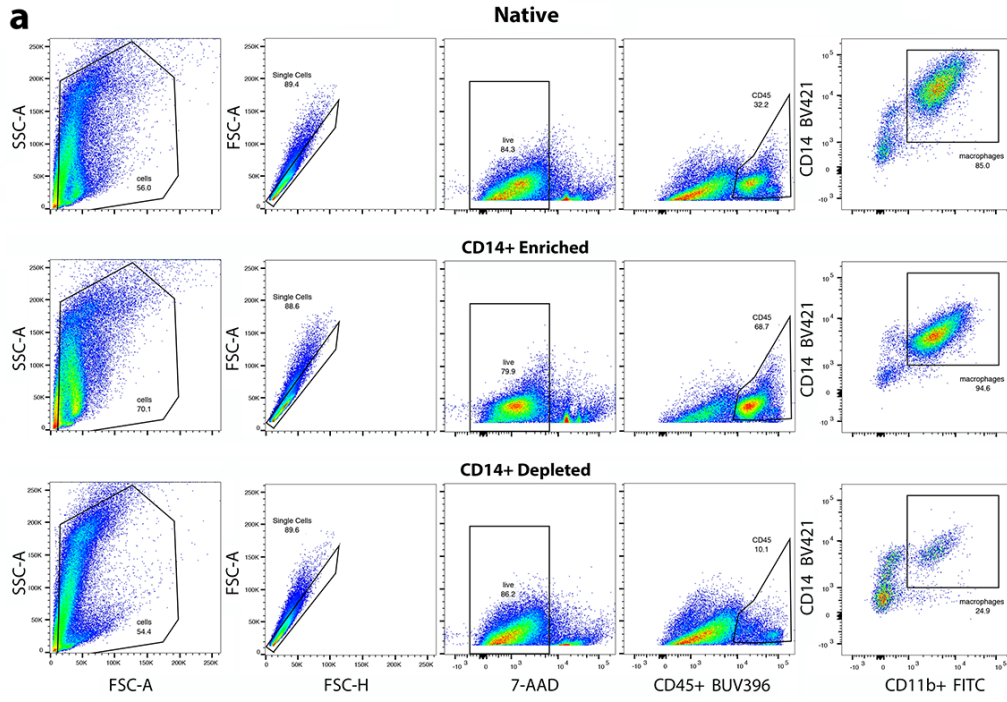
**Supplementary Figure 2, related to Figure 1d. Patient-specific heatmaps depicting fold-change induction from mock control for each cytokine.**

Only patients for which all 4 treatments were tested are shown (n=14); concentrations and experimental design are described in Figure 1.



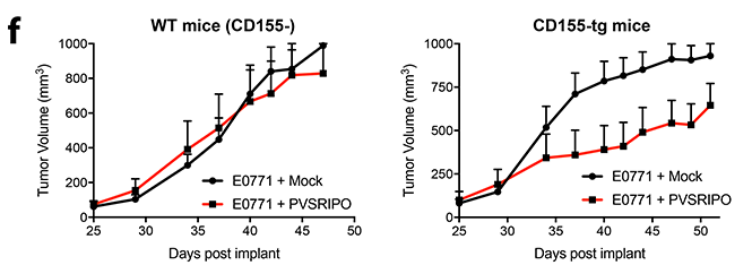
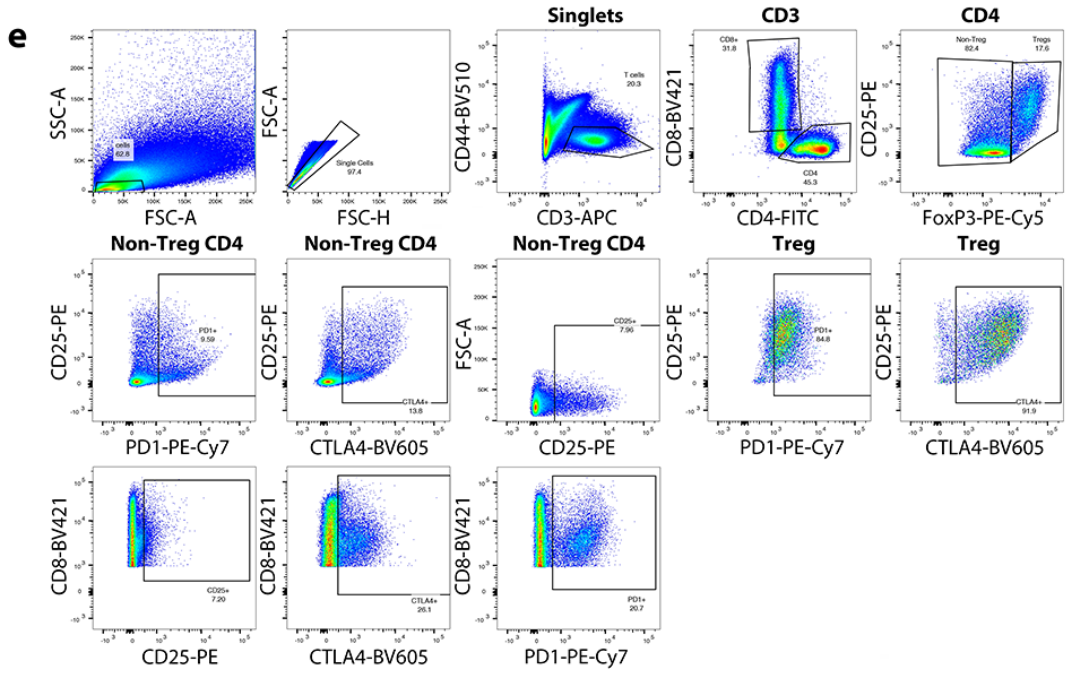
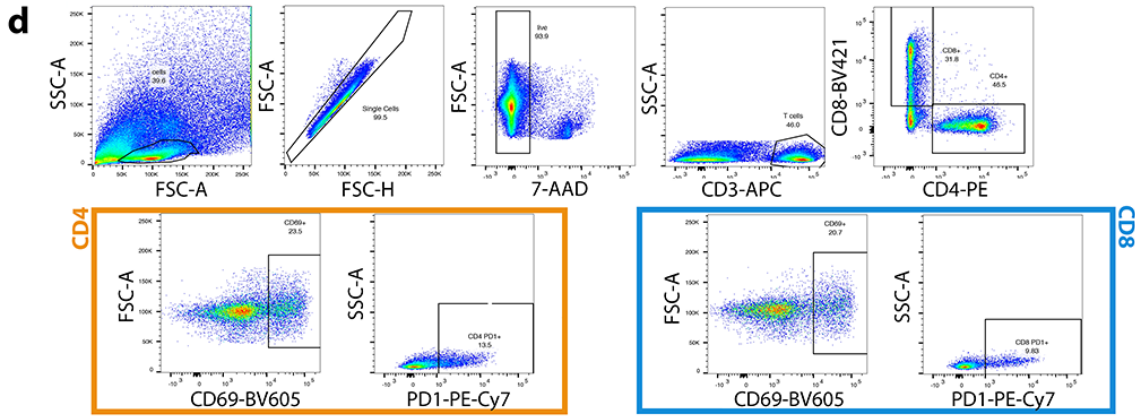
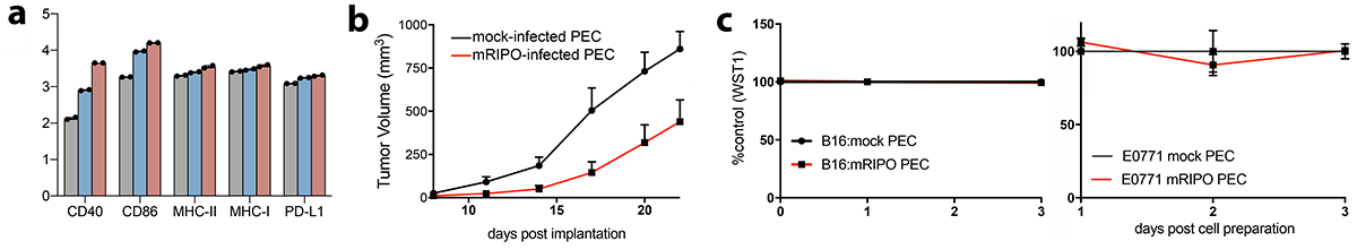
**Supplementary Figure S3, related to Figure 1f and g. Gating strategy for tumor-associated macrophage activation and IFIT1 status after in vitro slice culture assay.**

(a) Representative gating strategy for macrophage activation status in GBM and breast cancer specimens after *ex vivo* treatment (n=6 GBM, n= 2 breast cancer were tested); MFI (median fluorescence intensity) is shown on the x axis for histograms (bottom). (b) Post-treatment slice culture-derived tumor associated macrophages, endothelial cells, and tumor cells analyzed for PD-L1 in Figure 1f were also tested for CD40, CD86, HLA-DR; individual values are shown for each patient specimen and data brackets indicate mean  $\pm$  SEM (n=6 GBM). (c) Representative histograms for intracellular IFIT1 staining after gating performed as in (a); data from all tested samples (n=4 GBM, n=2 breast cancer) presented in Fig. 1g.



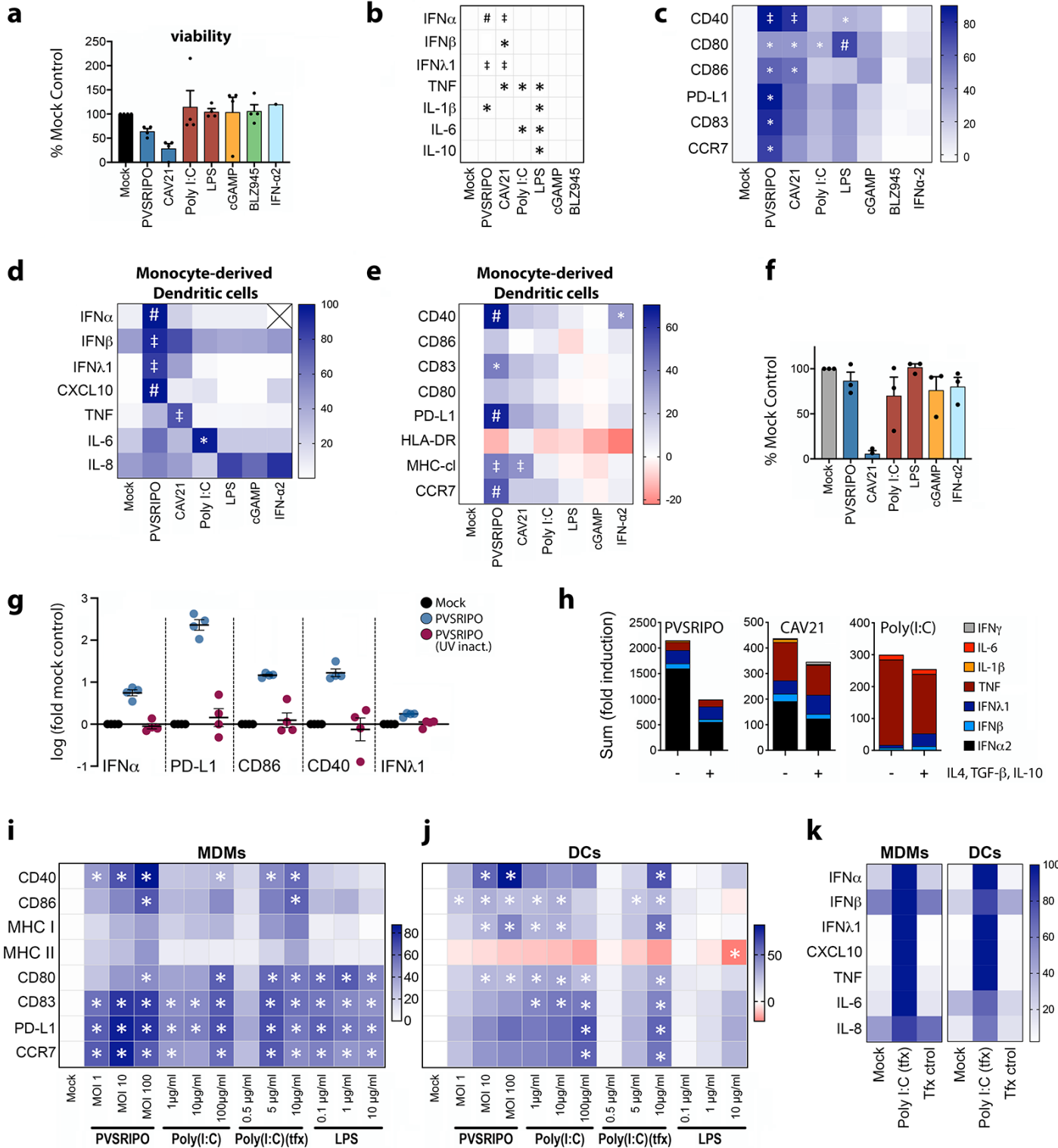
**Supplementary Figure S4, related to Figure 1g and h. Cytokine responses of tumor cell suspensions and PBMCs after PVSRIPO/PRR agonist treatment depend upon CD14+ myeloid cells.**

(a) Representative data assessing CD14+ cell enrichment/depletion for GBM single cell suspensions. (b) Individual data points for cytokine data presented in Figure 1h, including cytokine secretion from CD14+ cells (from n= 9 tumors). (c, d) Human PBMCs (n= 3 donors) were treated with mock or PVSRIPO after CD14+ pre-depletion, post-depletion, or CD14+ purified fractions, and tested for IFIT1 staining (c) as in Figure 1g, or supernatant cytokine analysis (d) as in Figure 1h; p-value is from paired t test (two-tailed) comparing sum fold-mock induction. (b-d) All data bars/brackets indicate mean  $\pm$  SEM.



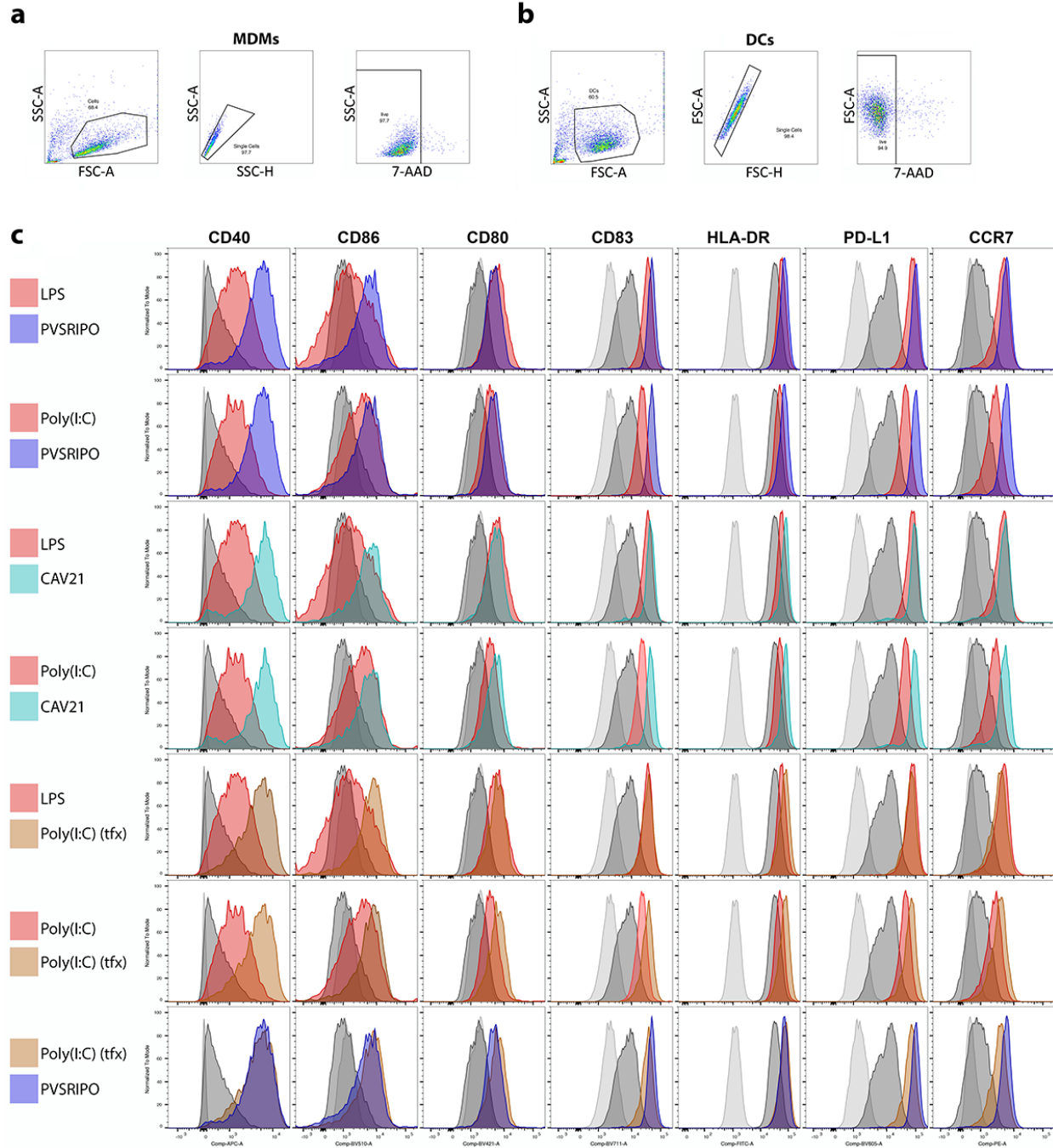
**Supplementary Figure 5, related to Figures 2 and 3. Murine myeloid cells and the non-malignant TME mediate antitumor efficacy in response to mRIPO infection.**

(a) Flow cytometry analysis of PEC treated with Mock (gray bars), mRIPO (MOI 10, blue bars) or LPS (100ng/ml, red bars) (24h), expressed as log MFI for each cell surface marker (n=2 experiments). (b) Repeat experiment for series presented in Figure 2b, left panel (B16, n= 10 mice/group); mean tumor volume + SEM is shown. (c) Tumor cell preparations used for implantation into mice in Figure 2b were plated in 96 well plates (1000 cells per well) and analyzed by WST1 assay for viability for 3 days; B16 (left panel) and E0771 (right panel), a representative series is shown from n=2 cell preparations per model; mean +/- SEM is plotted from technical replicates within one experiment. (d) Representative gating strategy for T cell panel testing CD69 and PD1. (e) Representative gating strategy used to determine Treg and non-Treg CD4 phenotypes in Figure 2c. (f) WT E0771 cells were co-implanted into the fat pad of WT (left panel) or CD155-tg (right panel) mice with or without  $1 \times 10^8$  pfu mRIPO; mean tumor volume and SEM is shown (left panel: n=4/group; right panel: n=10/group).



**Supplementary Figure 6, related to Figure 4. Enteroviral replication/cytoplasmic dsRNA induce a distinct type-I/III IFN dominant phenotype in human macrophages and DCs.**

(a) Viability determined by WST1 assay for MDMs after various treatments as shown in Figure 4a (n=4 experiments, except IFN $\alpha$ 2 which was tested in this assay once); mean + SEM is shown. (b) Tukey's post hoc test p<0.05 (two-tailed) comparing each individual treatment in Figure 4a to mock (\*), all other groups except PVSRIPO or CAV21 (‡), or (#) all other groups. (c) Flow cytometry analysis of activation markers on macrophages from Figure 4a (n=4 experiments/group except for cGAMP, BLZ945, and IFN $\alpha$ 2 where n=2); symbols indicate same statistical information as in (b), comparisons were not performed for cGAMP, BLZ495, or IFN $\alpha$ 2 due to n=2. (d-f) Cytokine (d), flow cytometry analysis (e), and viability (f, WST1 assay, data bars represent mean +/- SEM) of monocyte-derived DCs treated as in Figure 4a (d and e n=4, f n=3 experiments); symbols indicate same as in (b). (g) MDMs were treated with Mock, PVSRIPO, or UV-inactivated PVSRIPO and supernatant was assayed for cytokine release. Cell surface staining (PD-L1, CD86, CD40) was also performed; relevant cytokines and cell surface markers are shown (n=4 experiments from 2 different donors) normalized between experiments by determining log-fold mock control. Brackets indicate mean values and SEM. (h) Macrophages were differentiated with M-CSF alone or in combination with IL-4, TGF- $\beta$ , and IL-10 (all 20pg/ml) and treated with mock, PVSRIPO (MOI 10), CAV21 (MOI 10), or Poly(I:C) (10 $\mu$ g/ml). Cytokine release was measured and fold-mock control values were plotted together in each data bar to depict relative contribution to total cytokine induction (n=2 experiments). (i, j) Accompanying flow cytometry data for cells from experiments in Figure 4c (i) and 4d (j); %maximum MFI was determined followed by subtracting mock values for each activation marker; (\*) indicates Tukey's post hoc test p<0.05 (two-tailed) vs mock treatment. (k) Comparison of Poly(I:C)-TFX vs transfection reagent (lyovec) alone in MDMs and DCs as indicated; %maximum concentration is shown.



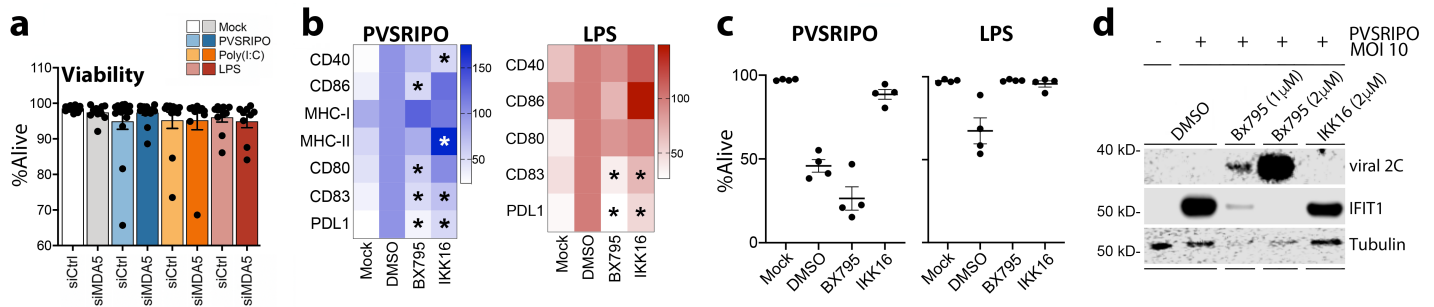
**Supplementary Figure 7, related to Figure 4. Analysis of surface activation marker phenotype after enterovirus/cytoplasmic dsRNA compared to TLR agonists.**

Gating strategy for MDMs (**a**) and DCs (**b**); histograms for surface activation markers on MDMs from a representative experiment (**c**).



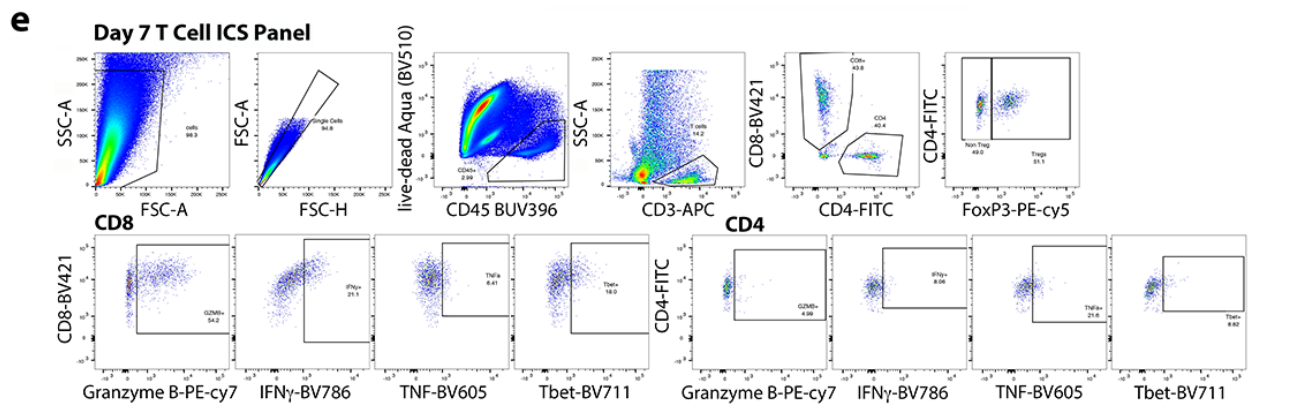
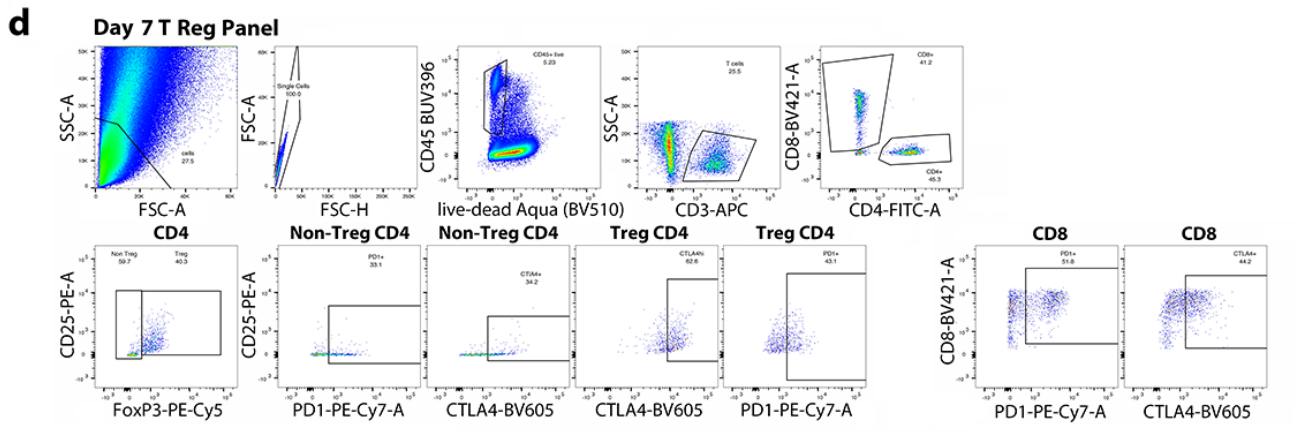
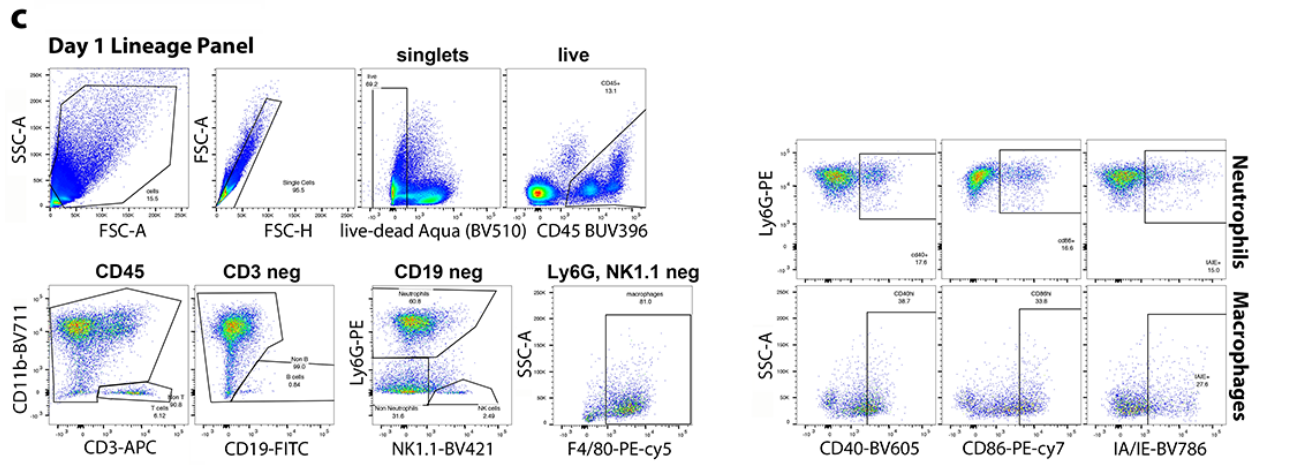
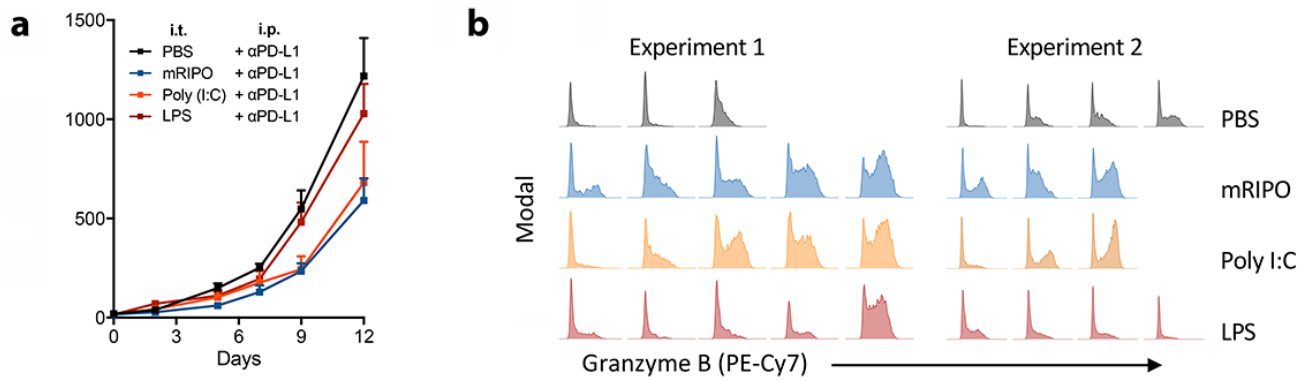
**Supplementary Figure 8, related to Figure 5. Immunoblots from 4 different donors, including all blots quantitated in Figure 5b.**

Each immunoblot series was performed once for each donor, with extended analysis performed for donor 1 (a). (b) Asterisk below p-IRF3 blot for donor 4 indicates a background band appearing below the true p-IRF3(S396) band, which was defined by ladder and detection of total IRF3 on a companion blot for all donors. N=4 experiments using 4 donors.



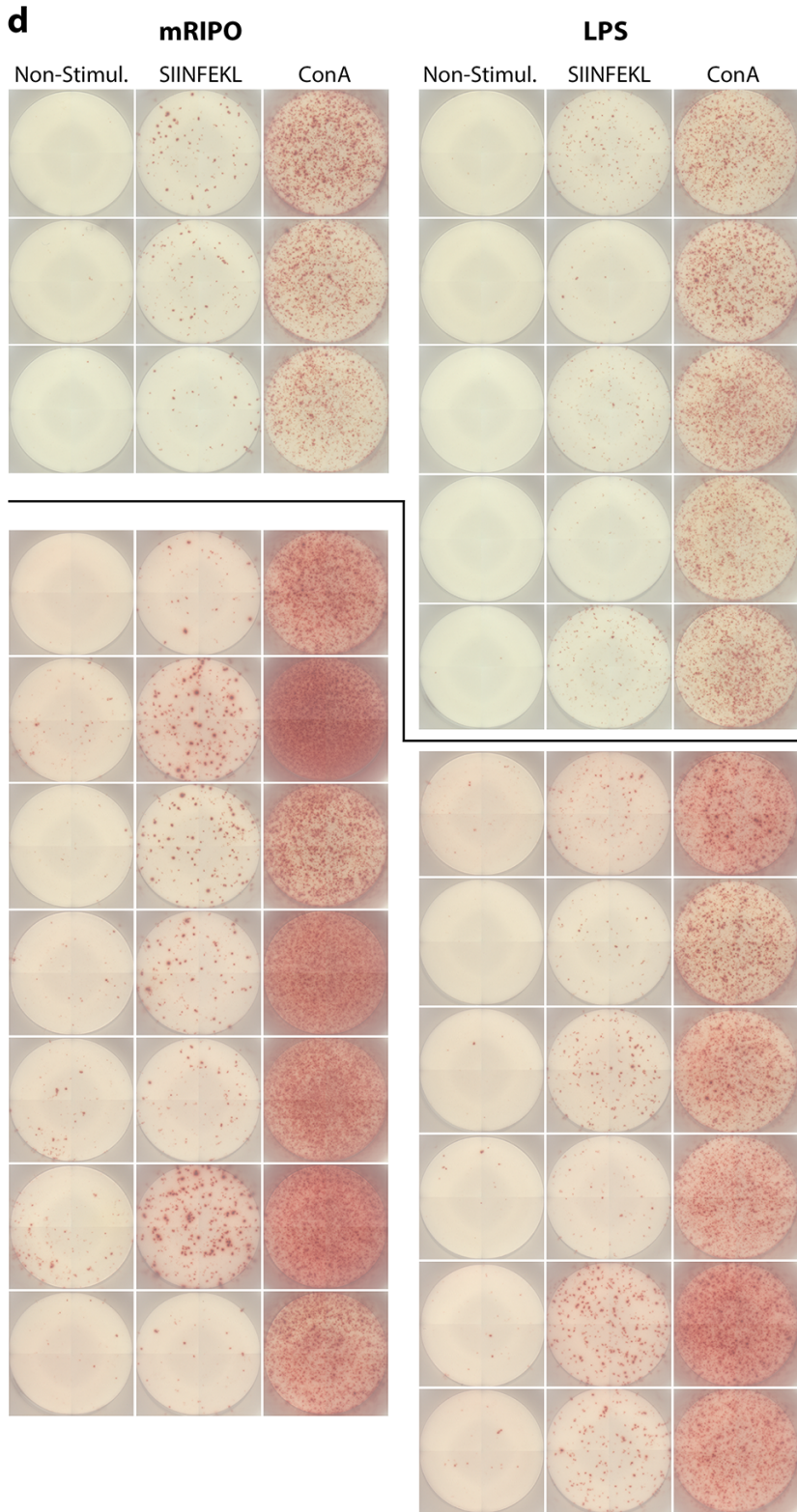
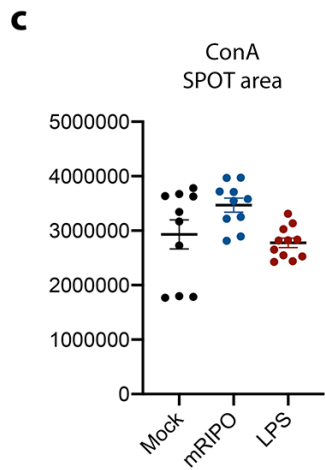
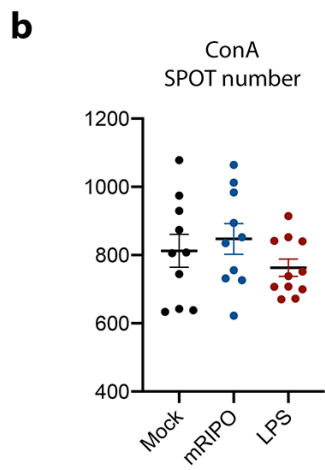
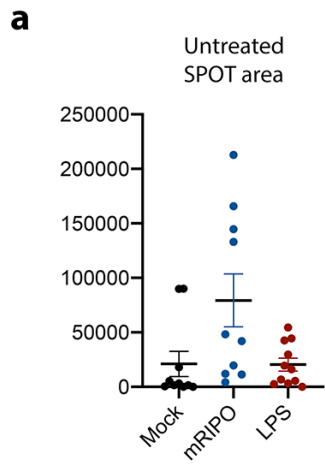
**Supplementary Figure 9, related to Figure 6. Macrophage activation phenotype after PVSRIPO infection depends upon MDA5-TBK1 signaling.**

(a) Cell viability by 7-AAD after control vs MDA5-targeting siRNA transfection, and stimulation with PVSRIPO/TLR agonists as shown in Fig. 6a-b (n=16 experiments PVSRIPO, n=10 LPS, n=12 all others; data bars represent mean  $\pm$  SEM). (b) Heatmaps depicting levels of cell surface activation markers, and (c) viability (7-AAD) on cells from experiments in Fig. 6c (n=4 experiments; data brackets indicate mean  $\pm$  SEM; (\*) indicates Tukey's post-hoc  $p < 0.05$  vs DMSO treatment control). (d) Immunoblot analysis of viral protein (2C) and IFIT1 in the presence and absence of Bx795 or IKK16 during PVSRIPO infection, a representative series from n=2 experiments is shown.



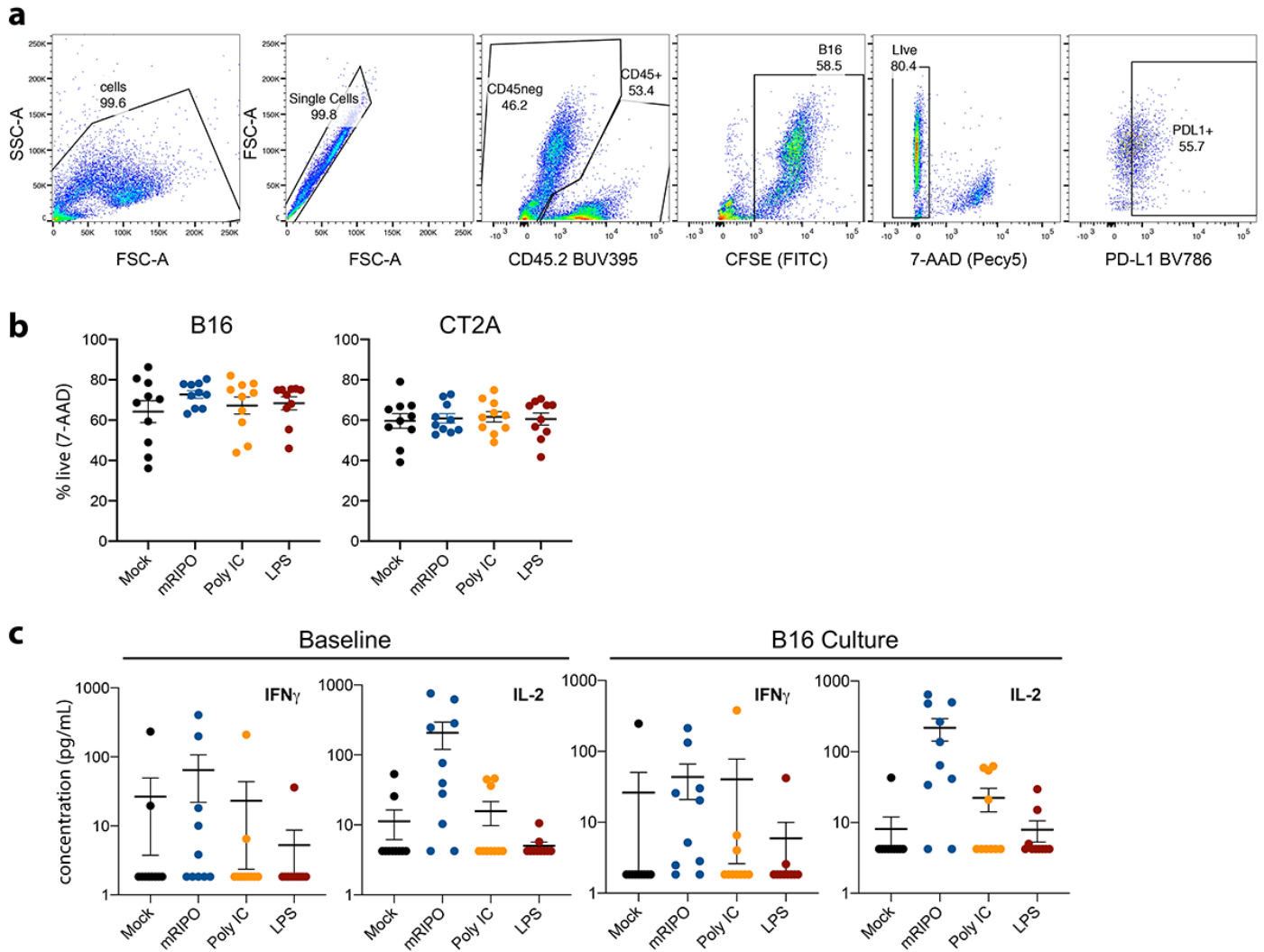
**Supplementary Figure 10, related to Figure 7. mRIPO therapy is associated with polyfunctional tumor infiltrating T cell phenotypes.**

(a) Repeat experiment for Figure 7a [n=5 for mRIPO/LPS, n=6 for PBS/Poly(I:C)]; mean tumor volume + SEM is plotted by treatment group. (b) Histograms of 2 experimental cohorts testing Granzyme B expression on CD8<sup>+</sup> T cells after PBS, mRIPO, Poly(I:C) or LPS treatment, corresponding to data in Figure 7e. (c) Representative gating for macrophages, neutrophils, and NK cells along with relevant activation markers presented in Figure 7e; isotype control staining was used to define CD40, CD86, and IA/IE positivity. (d) Representative gating for Treg panel testing Treg, non-Treg, and CD8<sup>+</sup> T cell expression of CTLA4 (intracellular stain), and PD1 in Figure 7e. (e) Representative gating for T cell panel assessing intracellular Granzyme B, IFN $\gamma$ , TNF- $\alpha$  and T-bet expression by T cells as shown in Figure 7e; isotype control stained fluorescence minus one samples were used to determine positive intracellular staining (Granzyme B, IFN $\gamma$ , TNF- $\alpha$ , and T-bet) populations.



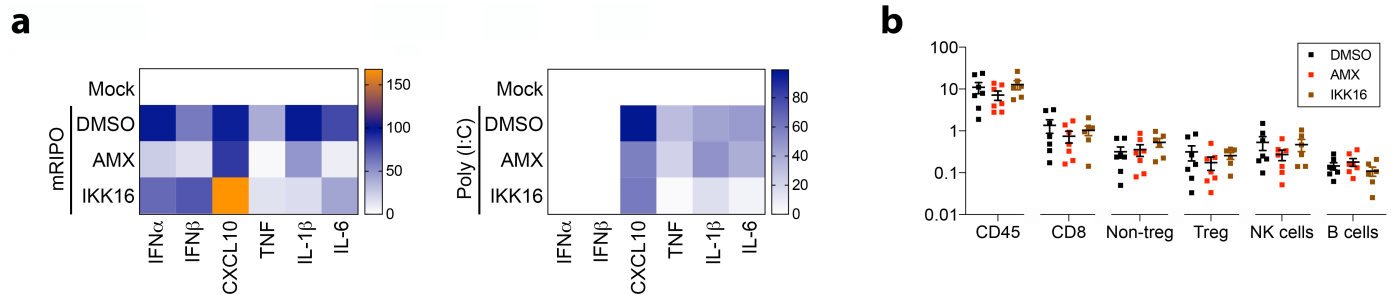
**Supplementary Figure 11, related to Figure 8b. Additional analyses for ELISpot data presented in Figure 8b.**

(a) Baseline total spot area for non-stimulated splenocytes. (b) Spot numbers for positive control (concanavalin A) treated splenocytes for ELISpot data presented in Figure 8b. (c) Total IFN $\gamma$  spot area after Concanavalin A stimulation of splenocytes. (a-c) n=10 mice for PBS/mRIPO, n=11 mice LPS pooled from 2 experiments; data brackets indicate mean  $\pm$  SEM. (d) Scans of ELISpot plates using splenocytes from tumor-bearing mice treated with mRIPO or LPS; the panels above and below the bar represent two independent experiments. In all ELISpot graphs/pictures all values for the mice with the 2 highest and 2 lowest IFN $\gamma$  spot counts after SIINFEKL stimulation were excluded from each group to eliminate outliers; thus, the same samples (from the same mice) were excluded from all panels.



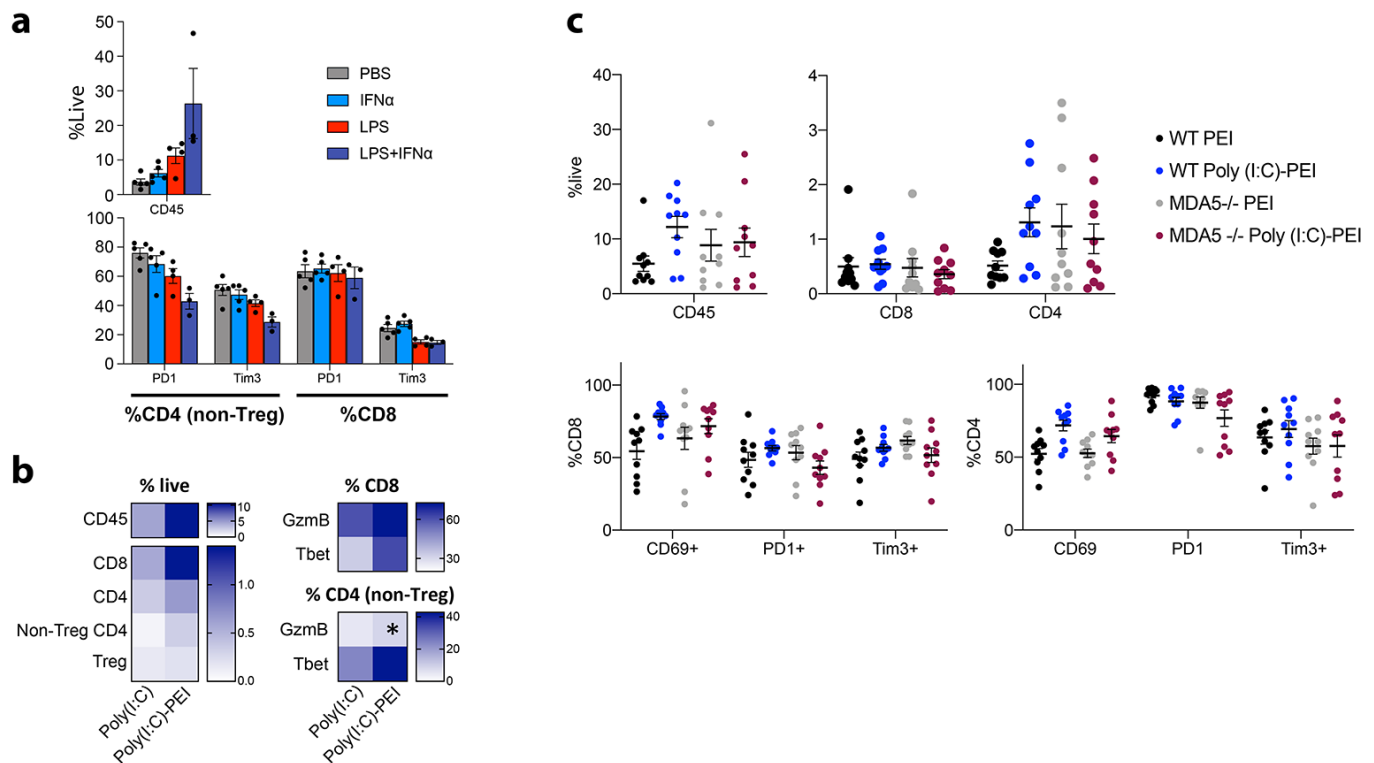
**Supplementary Figure 12, related to Figure 8d. Analysis of TDLN:B16 co-cultures seven days after mRIPO vs TLR agonist therapy.**

(a) Gating strategy for CFSE and PD-L1 analysis in Figure 8d. (b) %Live B16 and CT2A cells after TDLN cell co-culture presented in Figure 8d as measured by 7-AAD. (c) Supernatant cytokines were measured after 48h TDLN cell:B16 or CT2A co-culture from Figure 8d. (b, c) Data brackets represent mean  $\pm$  SEM; n=10 mice per group.



**Supplementary Figure 13, related to Figure 9a, b. Confirmation of AMX inhibitor activity in murine cells and extended analysis of immunological changes after TBK1 inhibition.**

(a) Heatmaps presenting cytokine release (24h) of DMSO, Amlexanox (2.5 $\mu$ M), or IKK16 (50nM) treatment of FLT3L-derived BMDCs in the presence of mRiPO (left, MOI 10) or Poly(I:C) (right, 10 $\mu$ g/ml). Percent maximum cytokine concentration (pg/ml) was determined, mock values were subtracted; mean normalized values are plotted [n=2 experiments]. (b) Extended analyses for tumor infiltrating cell type density (%live cells) for each indicated cell type for the experiment presented in Figure 9a. Data brackets represent mean  $\pm$  SEM; n= 7/group mRiPO + DMSO and AMX, n=6 for mRiPO + IKK16.



**Supplementary Figure 14, related to Figure 9e, g, and i. Type-I IFN and cytoplasmic Poly(I:C) potentiate intratumor inflammation and T cell activation.**

(a) Extended associated flow cytometry analyses for experiment performed in Figure 9e (n=3 mock/LPS + IFN $\alpha$ , n=5 IFN $\alpha$ , n=4 LPS only). (b) Tumors were harvested from surviving mice 16 days after treatment in the experiment described in Figure 9g and analyzed for immune infiltrates/T cell phenotypes [n=3 Poly(I:C), n=7 Poly(I:C)-PEI]; (\*) t-test (two tailed) comparing Poly(I:C) vs Poly(I:C)-PEI, p=0.047. (c) Extended flow cytometry analyses for Figure 9i (n=10 mice/group). (a, c) All brackets/data bars represent mean  $\pm$  SEM.